STUDIA UBB PHYSICA, Vol. 67 (LXVII), 1-2, 2022, pp. 17-24
(RECOMMENDED CITATION)
doi:10.24193/subbphys.2022.02

INVESTIGATION OF THE PHYSICAL PROPERTIES OF $MnNi_{(1-X)}M_X$ ALLOYS WHERE M=Ti, Al

R. HIRIAN[1], A. MERCEA[1], V. POP[1*]

ABSTRACT. $Mn_{50}Ni_{50-x}M_x$, where M= Ti, Al and x=0, 2.5, 5 and 10, alloys with the L10 crystal structure were successfully synthesized. The martensite type transformation was fond to be strongly affected by doping. Both x=10 samples show a spin glass type behavior while the sample doped with Al also shows large exchange bias.

Keywords: *hard magnetic materials, Mn based alloys, exchange bias, spin glass.*

INTRODUCTION

Permanent magnets are crucially important for modern industry. The high energy product $Nd_2Fe_{14}B$ and highly stable $SmCo_5$ or Sm_2Co_{17} based magnets permit the creation of highly compact devices, such as mobile phones and laptops, while also being excellent at delivering high performance for large applications such as wind turbines and electric vehicles [1-6]. However, the supply of rare-earth elements is tenuous and their extraction and processing has significant environmental impact, therefore a concerted scientific effort has been put forward in recent years towards developing magnetic materials from non-rare earth elements [4]. Amongst the proposed solutions are Mn based phases [2, 4], such as MnBi [7] and MnAl [8, 9], as they are low cost and present good magnetic properties. The useable magnetocrystalline anisotropy of these materials is given by the L10 crystal structure with high *c/a* ratio. In this work, we study the effect of doping on the L10 MnNi phase [10]. While this phase is antiferromagnetic, adequate doping may change the Mn-Mn distance leading to ferromagnetic coupling, similar to MnAl or MnBi.

[1] *Faculty of Physics, Babeş-Bolyai University, Cluj-Napoca, RO-400084 Romania*
** Corresponding author: viorel.pop@ubbcluj.ro*

EXPERIMENTAL

The $Mn_{50}Ni_{50-x}M_x$, where M=Ti, Al and x=0, 2.5, 5 and 10, alloys were produced by induction melting of the pure elements under purified argon atmosphere. The as-cast ingost were then placed in tantalum sample holders inside evacuated cuartz tubes and annealed at 1000 K for 48 h. In order to preserve formation of the high temperature structure, the samples were quenched in water.

Crystalline structure of the produced material was investigated using X-ray diffraction (XRD), on a Bruker D8 Advance diffractometer equipped with a Cu Kα source. The lattice parameters were calculated from XRD patterns using the Celref3 program.

Differential scanning calorimetry (DSC) measurements were carried out on a TA-Instruments Q600 simultaneous thermal analysis instrument. Measurements were done in high purity Ar flow, with a heating and cooling rate of 20 ^{o}C/min.

Thermomagnetic measurements were carried out on a Faraday-Weiss type magnetic balance, in the temperature range 300-900 K.

Magnetization measurements, along with zero-field cooled (ZFC) and field cooled (FC) measurements up to room temperature, were carried out using a vibrating sample magnetometer produced by Cryogenics.

RESULTS AND DISCUSSION

In order to determine the annlealing temperature of the $Mn_{50}Ni_{50-x}M_x$ alloys, DSC measurements were carried out in the temperature range between 600 K and 1100 K, *Figure 1*. These measurements show a phase transition around 1000 K for the undoped MnNi phase. This transition corresponds to the martensitic transformation between the low temperature and high temperature MnNi phase [10, 11]. In the case of both Ti and Al doping, *Figure 1a and 1b* respectively, we can see that the martensitic transformation shifts to lower temperature as doping is increased. The transformations for the x=10 samples are shifted below the measurement range of the instrument, i.e. below 600 K.

In order to obtain the L10 phase at room temperature, all samples were annealed for 48 h at 1000 K and quenched.

The X-Ray diffraction patterns for the annealed and quenched alloys are given in *Figure 2.* In the case of Al doping, *Figure 2b*, the structure of the L10 MnNi alloys is maintained for all doping ammounts. Of note are the shifts in peak

possitions due to the variations of lattice parameters. In the case of Ti doping, *Figure 2a*, the majority phase is the L10 MnNi phase, however some impurity peaks can bee seen for x=2.5 and x=10, to the right of the very intense [101] peak.

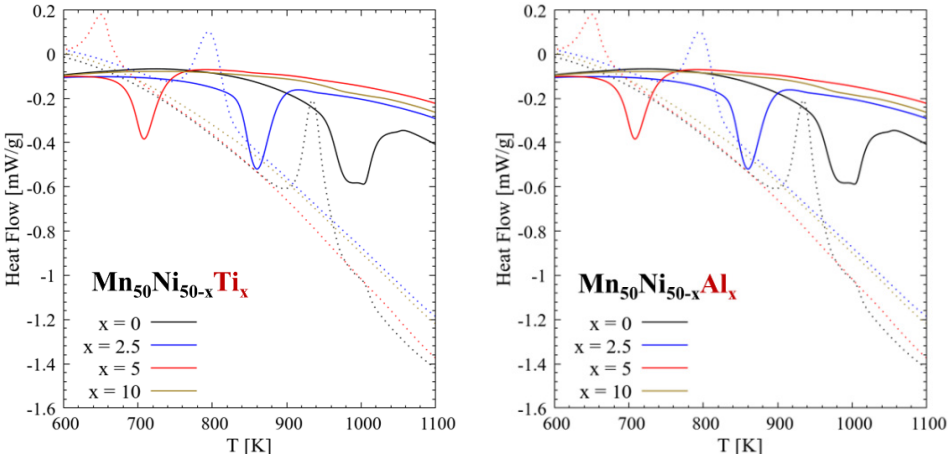

(a) (b)

Figure 1. DSC curves for $Mn_{50}Ni_{50-x}M_x$ alloys, where M is Ti (a) or Al (b). Cooling curves are dashed. Exotherms are displayed as peaks.

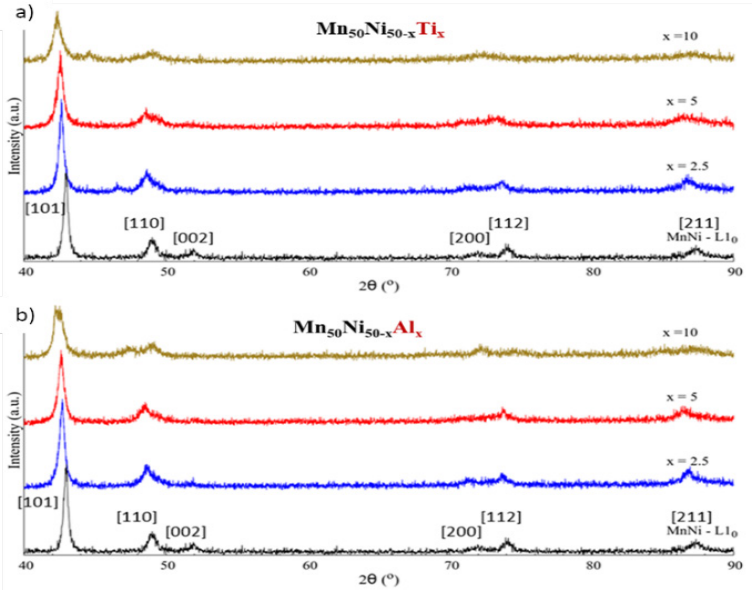

Figure 2. X-Ray diffraction patterns for the annealed and quenched $Mn_{50}Ni_{50-x}M_x$ alloys, where M is Ti (a) or Al (b).

The lattice paramenters for the doped alloys were estimated from XRD, using the space group P4/mmm, Table 1. For Al doping, the *a* parameter remains largely unchanged until x=10, when it contracts slightly. On the other hand, the MnNi cell is expanded on the *c* axis when Al is entered into the structure. This expansion cause an increase in the c/a ratio from 1.34 at x=0 to 1.40 at x=10. In the case of Ti doping, the same trend is observed, a significant contraction of the *a* parameter alongside an expansion of the *c* parameter for x=10.

Table 1. Lattice parameters, estimated from XRD, for the annealed and quenched $Mn_{50}Ni_{50-x}M_x$ alloys, where M is Ti or Al.

Composition	a (Å)	error	c (Å)	error	c/a ratio
x=0	2.641	0.008	3.534	0.003	1.34
M=Al x=2.5	2.641	0.016	3.541	0.014	1.34
M=Al x=5	2.655	0.005	3.557	0.004	1.34
M=Al x=10	2.632	0.003	3.681	0.031	1.40
M=Ti x=2.5	2.647	0.006	3.538	0.006	1.34
M=Ti x=5	2.648	0.040	3.556	0.013	1.34
M=Ti x=10	2.628	0.061	3.608	0.057	1.38

Thermomagnetic measurements (*Figure 3*) are in accordance with the DSC measurements, with magnetic transitions associated with the structural transformations, being measured around 900 K and 800 K for the samples with x=2.5 and x=5 respectively. It should be noted, that the thermomagnetic measurement range is larger than that used in DSC, *Figure 1*, therefore all of the phase transitions can be investigated. The Ti and Al doping at x=10 reduces the phase transition temperature to aproximately 400 K. In all cases, for the magnetic transitions, hysteresis is observed, which can be explained by the thermodynamics of phase transitions, specifically the undercooling and superheating imposed by the germination process.

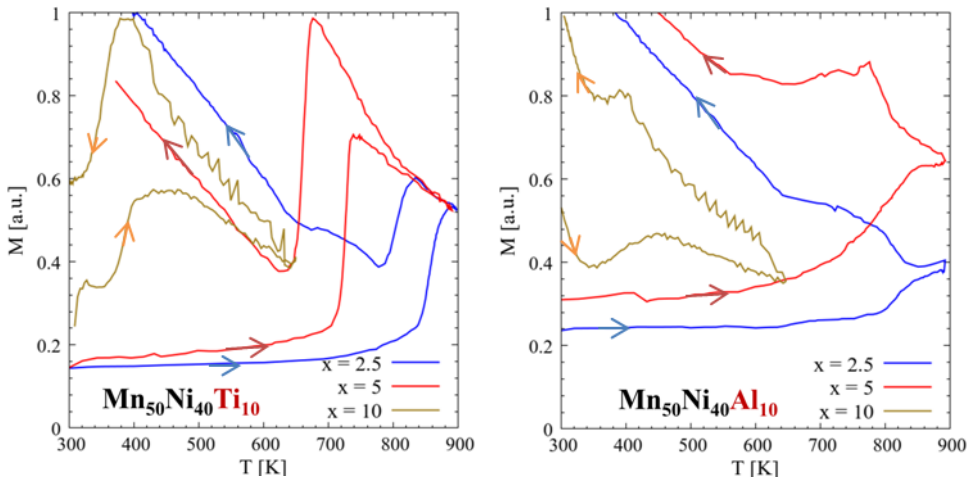

(a) (b)

Figure 3. Thermomagnetic measurements in small applied magnetic field, between 300 K and 900 K, for the annealed and quenched $Mn_{50}Ni_{50-x}M_x$ alloys, where M is Ti (a) or Al (b).

ZFC and FC curves for the x=10 alloys are shown in *Figure 4*. For the Ti doped alloy, *Figure 4a*, we see a large diffrence between the FC and ZFC curves, at low temperatures. The blocking temperature for these alloys is close to 70 K. In the case of Al doping, *Figure 4b*, while we still see a large difference between the ZFC and FC curves, the blocking temperature is much higher, around 140 K. At room temperature, a small peak appears, possibly a Neel temperature. Moreoever, this feature seems to show signs of thermal hysteresis. In the case of Al doping, similar low temperature features were observed to be due to a spin glass type behaviour [12]. Due to the similarity of the behaviour and composition, we may suspect that there is possible spin glass behaviour in the Ti doped sample as well.

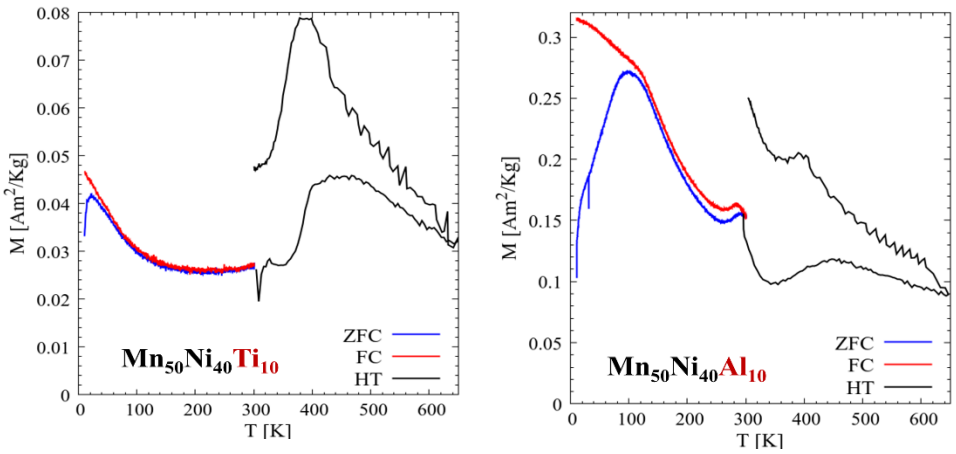

(a) (b)

Figure 4. ZFC and FC curves concatenated with high temperature measurements (HT) for the annealed and quenched $Mn_{50}Ni_{40}M_{10}$ alloys, where M is Ti (a) or Al (b).

Magnetization measurements for the x=10 samples are given in *Figure 5*. The samples measured at 4 K have been field cooled. Measurements at 4 K, for the Al doped sample (*Figure 5b*) show the existence of a large exchange bias, typical of the coexistence of ferromagnetic and antiferromagnetic interactions. The exchange bias disappears at high temperature, 300 K and 500 K. At elevated temperature, although the behaviour seems largely paramagnetic, the slight change in slope around 0 T indicates the presence of some non-compensated negative magnetic interaction.

The analysis of the magnetization curves is also similar to that of Ti doping at high temperature (*Figure 5a*) however the exchange bias seen at 4 K in the case of Al doped samples completely disappears when doping with Ti. At higher temperatures, the Ti doped samples show some magnetic order, likely due to uncompesate negative magnetic interactions.

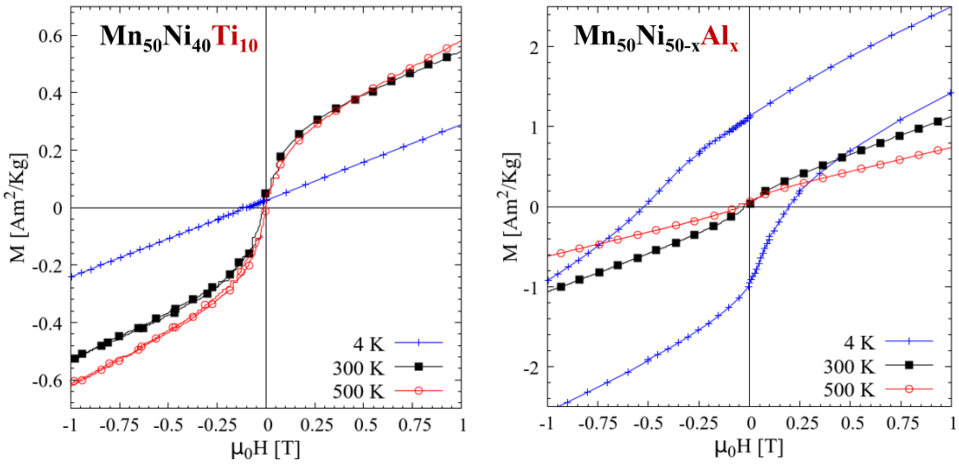

Figure 5. Magnetization measurements at 4 K, 300 K and 500 K, for the annealed and quenched $Mn_{50}Ni_{40}M_{10}$ alloys, where M is Ti (a) or Al (b).

CONCLUSIONS

$Mn_{50}Ni_{50-x}M_x$, where M= Ti, Al and x=0, 2.5, 5 and 10, alloys with the L10 crystal structure were successfully synthesized. Both Ti and Al doping produces distorsions of the L10 MnNi lattice. At doping amounts of x=10, the *c/a* ratio is significantly increased.

Doping also lowers the martensite transformation temperature, from 900 K for x=0 to 400 K for x=10.

In the case of $Mn_{50}Al_{40}M_{10}$ alloys, for both M=Ti and M=Al doping, the samples show a spin glass type behaviour at low temperatures.

The $Mn_{50}Al_{40}Al_{10}$ alloys show a large exchange bias at low temperatures. This feature is absent in the Ti doped sample.

AKNOWLEGEMENT

This work was made possible through the financial support of the Romanian Ministry of Research, Innovation and Digitalization, grant PN-III-P2- 2.1-PED-2019-4696.

REFERENCES

[1] D. Sander, S. O. Valenzuela, D. Makarov, C. H. Marrows, E. E. Fullerton, P. Fischer, J. McCord, P. Vavassori, S. Mangin, P. Pirro, et al. *J. Phys. D. Appl. Phys.* 50 (2017), doi:10.1088/1361-6463/aa81a1.

[2] J.M.D. Coey, *IEEE Trans. Magn.* 47, 4671-4681, (2011) doi:10.1109/TMAG.2011.2166975.

[3] D. Goll, H. Kronmüller,*Naturwissenschaften* 87, 423-438, (2000) doi:10.1007/s001140050755.

[4] J. M. D. Coey, *Engineering* 6, 119–131, (2020) doi:10.1016/j.eng.2018.11.034.

[5] N.T. Nassar, X. Du, T.E. Graedel, *J. Ind. Ecol*. 19, 1044–1054, (2015) doi:10.1111/jiec.12237.

[6] K. Binnemans, P.T. Jones, B. Blanpain, T. Van Gerven, Y. Yang, A. Walton, M. Buchert, *J. Clean. Prod.* 51, 1–22, (2013) doi:10.1016/j.jclepro.2012.12.037.

[7] R. Hirian, R. Dudric, O. Isnard, K. Kuepper, M. Coldea, L. Barbu-Tudoran, V. Pop, D. Benea, *J. Magn. Magn. Mater*. 532, 167997, (2021), doi:10.1016/j.jmmm.2021.167997

[8] S. Mican, D. Benea, R. Hirian, R. Gavrea, O. Isnard, V. Pop, M. Coldea, *J. Magn. Magn. Mater*. 401, 841-847, (2016), doi: 10.1016/j.jmmm.2015.11.011

[9] R. Gavrea, R. Hirian, S. Mican, D. Benea, O. Isnard, M. Coldea, V. Pop, *Intermetallics*, 82, 101-106, (2017), doi: 10.1016/j.intermet.2016.11.012

[10] E. Kren, E. Nagy, I. Nagy, L. Pal, P. Szabo, *J. Phys. Chem. Solids*, 29, 101-108, (1968), doi:10.1016/0022-3697(68)90259-X

[11] V. Rednic, M. Coldea, S.K. Mendiratta, M. Valente, V. Pop, M. Neumann, L. Rednic, *J. Magn. Magn. Mater*. 321, 3415-3421, (2009) doi: 10.1016/j.jmmm.2009.06.020

[12] H. Pan, Li Ma, G. K. Li, L. Y. Jia, C. Zhen, D.-L. Hou, W. Wang, E. Liu, J. L. Chen, G.H. Wu, *Intermetallics*, 86, 116-120, (2017) doi:10.1016/j.intermet.2017.03.003